Unequal-Sphere Packing Model for Simulation of the Uniaxially Compressed Iodine Adlayer on Au(111)

Alexandre Tkatchenko and Nikola Batina*

Laboratorio de Nanotecnologia e Ingenieria Molecular, Area de Electroquimica, Departamento de Quimica, CBI, Universidad Autonoma Metropolitana Iztapalapa, Av. San Rafael Atlixco No. 186, Col. Vicentina, Del. Iztapalapa, C.P. 09340 Mexico, D.F., Mexico

Received: May 20, 2005; In Final Form: August 18, 2005

A simple unequal-sphere packing (USP) model, based on pure geometrical principles, was applied to study the centered-rectangular iodine c($p\times\sqrt{3}$)*R*30° adlayer on the Au(111) surface, well-known from surface X-ray structure (SXS), low energy electron diffraction (LEED), and scanning tunneling microscopy (STM) experiments. To reproduce the exact patterns observed in experiments, two selective conditions—minimum average adsorbate height and minimum adlayer roughness—were imposed. As a result, a series of adlayer patterns with c($p\times\sqrt{3}$)*R*30° symmetry ($2.3 < p < 3$), with precise structural details, including atomic registry and identification of the *p*-bisector as the most likely trajectory for the iodine adatom movement during the so-called *uniaxial compression* phenomenon, were identified. In addition, using the same model, the difference between the iodine adlayer arranged in hexagonal and centered-rectangular c($p\times\sqrt{3}$)*R*30° patterns, as in the case of Pt(111) and Au(111) surfaces, was investigated. Qualitative and quantitative comparison shows that iodine adatoms in these two arrangements differ significantly in atomic registry, distance from the substrate, and the adlayer corrugation. Our findings could be of special interest in the study of the nature of the iodine adatom bonding to different substrates (i.e., Au vs Pt).

Introduction

Halide adsorption phenomena have for a long time been a preferred subject of different studies in modern surface science and electrochemistry.[1−3] Special interest in characterization of the anion adlayers on metal surfaces is related to fundamental issues, as it is the structure of the electrode double layer and from a practical technological importance (i.e., corrosion). In particular, the progress becomes obvious after use of electrodes with well-defined surfaces, electron spectroscopies such as low energy electron diffraction (LEED) and Auger,[1,4−6] and new techniques for characterization and visualization of the adsorbed layers with atomic resolution, such as scanning tunneling microscopy (STM), atomic force microscopy (AFM), and surface X-ray structure (SXS).[3] As a result, nowadays, we have a clear idea and evidence of different types of halide structures on metal surfaces such as Au(111), Ag(111), and Pt(111). Indeed, our interest and knowledge is expanded further than just adlayer structure characterization, to thermodynamics, anion−metal interactions, and other physical and chemical properties. Although it seems that the anion−metal interface (particularly at the well-defined substrate surface) becomes a very familiar system, and in many cases characterized with extraordinary precision at the atomic level, still it is very much unexplored from the technological point of view. Indeed, this could change by future development of nanoelectronics and nanodevices design with atomic level assemblies. However, it will require development of better models and identification of exact adatom registry as well as finding mechanisms which allow adatoms to be freely manipulated or transform from one kind of adlayer arrangement into another (phase transitions). So far, simulation of the anion adsorption is a difficult task due to the large number of atoms usually involved in description of such phenomena and insufficient computational capacity.[3]

Iodine on Pt(111) and Au(111) has been studied extensively in electrochemical and surface science communities, with a large number of published reliable data with respect to adlayer structure. In the case of the iodine adlayer on Pt(111), numerous studies agree on reported structures (in situ and ex situ characterization) of the iodine adlayer and chemisorption type of bonding to the Pt(111) surface.[7−9] Independent of the mode of preparation, under ultrahigh vacuum (UHV) conditions (vapor evaporation) or by electrochemical methods, the same characteristic structures were found. Theoretical studies related to I−Pt(111) are rare so far. In one of our papers, we demonstrated how these characteristic iodine adlayer structures could be successfully predicted and described by our homemade unequal-sphere packing (USP) model.[10] Also, recent ab initio density functional theory (DFT) calculation offers some new insights into the chemical nature of the iodine−Pt(111) bonding.[11]

Iodine on Au(111), which is the subject of this study, is very different from the I−Pt(111) system because of the phenomenon of the uniaxial compression as a result of the increase of the adsorbate surface coverage.[12] Such behavior makes this system significantly more complex than I−Pt(111), both from experimental and theoretical points of view. The history of the I−Au(111) investigation is very interesting, involving reports of many different iodine adlayer structures. The breakthrough came with the study of Ocko and co-workers[13] (SXS), which identified two incommensurate iodine adlattices—c($p\times\sqrt{3}$)*R*30° and "rot-hex"—and clearly demonstrated that a centered-rectangular iodine adlayer was formed via the uniaxial compression (electrocompression) mechanism. The c($p\times\sqrt{3}$)*R*30° structure was defined by the value of p (2.73−2.45), with a corresponding surface coverage (0.366−0.409) and iodine−

* Corresponding author. E-mail: bani@xanum.uam.mx.

10.1021/jp052662m CCC: $30.25
Published on Web 10/26/2005

iodine interatomic distance between 4.62 and 4.32 Å, respectively. The c($p\times\sqrt{3}$)*R*30° adlayer is incommensurate with gold atom rows along the principal direction and commensurate along the orthogonal ($\sqrt{3}$) direction. It is important to mention that in terms of the iodine−gold interlayer spacing, it was estimated that in the c($p\times\sqrt{3}$)*R*30° arrangement it is between 2.3 and 2.4 Å, which indicates the covalent nature of the iodine−gold bonding.[13] The c($p\times\sqrt{3}$)*R*30° transforms into the rot-hex arrangement at higher surface coverages.[14−23] Additional structural details of I−Au(111) were revealed by LEED and STM analysis.[24,25] STM shows the same iodine c($p\times\sqrt{3}$)*R*30° adlattices, which appear to be atomically flat. Note that "flatness" was exclusively observed from STM data. Using a simple geometrical model, in the same work, it was proposed that, during the uniaxial compression, iodine adatoms move along specific *p*-bisectors. Contrary to SXS[13] analysis, the LEED and STM data pointed to the existence of the ($\sqrt{3}\times\sqrt{3}$)*R*30° iodine adlayer, too. It is important to mention that, in these experiments, as well as in the SXS work, the iodine modification of the Au(111) was carried out from aqueous solutions under the electrode potential control. However, identical LEED patterns which correspond to c($p\times\sqrt{3}$)*R*30° and rot-hex structures were observed many years ago in the study of Cochran and Farrell,[26] where iodine adlayers on the Au(111) were prepared from I_2 vapor. Afterward, it was confirmed by Huang and co-workers[27] that I_2 vapor deposition forms the same structures as those found by Ocko (electrochemical preparation).[13] This relates the c($p\times\sqrt{3}$)*R*30° and rot-hex structures and the uniaxial compression phenomenon to iodine adlayer behavior on the Au(111) surface (results of the specific iodine−gold and iodine−iodine interactions) rather than the influence of the applied electrode potential. Note that electrocompression behavior in anion adlayers was also observed for several other systems, such as Br and Cl on Au(111),[20,29] and some useful physical models have been proposed to explain the origin of the driving force (lateral interactions between adsorbates) for such behavior.[30]

Here, we intend to characterize the I−Au(111) system by use of our newly developed USP model, which was successfully applied for characterization of I−Pt(111). In this previous study, to select the most likely iodine adlayer arrangements on the Pt(111) substrate, a single parameter, defined as the *average adsorbate height*, was used as a selective criterion. The iodine adlayer structures found in our simulation were identical to those reported in the literature, which proved the validity of our approach. However, when the same model was applied to the I−Au(111) system, no resemblance with experimental structures was achieved. Detailed analysis indicated the insufficiency of the minimum average adsorbate height as a single parameter in the process of selection of the most likely structures of the iodine adlayer on Au(111). Then, the question was, how many and which parameters need to be introduced into our USP model to be able to simulate systems of such great complexity, which includes the formation of c($p\times\sqrt{3}$)*R*30° and the uniaxial compression phenomenon. Surprisingly, we found that introduction of one additional parameter—the requirement of maintaining the minimum adlayer roughness—allows the USP model to become a suitable tool for such a difficult task. Thus, in the case of the I−Au(111) system, we present a new development of the USP model, based on the use of two selective parameters—minimum average height and minimum roughness of the adsorbed adlayer—which allows us to perform the characterization of the c($p\times\sqrt{3}$)*R*30° arrangement in great detail in a large range of *p* values. Using this particular model, we were able to repeat all structural characteristics well-known from the experimental studies as well as to determinate the exact registry of each iodine adatom and direction of the iodine adatom movement during the uniaxial compression. The validation of our approach and our way of modeling is once again confirmed due to the fact that we were able to reproduce and characterize the experimentally found structures.[13] Furthermore, comparison between the I−Au(111) and I−Pt(111) systems leads to a better understanding of differences in the adlayer structures and transitions between different arrangements, which is certainly promising for the design of future nanometric devices. Note, as was demonstrated before, the I−Au(111) system is a very promising substrate for the formation of highly ordered molecular arrays for use in molecular electronics,[31−34] which raises additional interest and necessity for detailed characterization of this particular system.

Methodology

To analyze the c($p\times\sqrt{3}$)*R*30° structures in great detail, the USP model,[10] developed recently in our laboratory and described in detail before, has been employed. It is based on modeling of the geometrical arrangement of unequal spheres (hard-ball contact model) over the crystalline substrate. The homemade software atomic level surface assembler (ALSA)[35] is used to perform simulations. ALSA allows the simulation of single or multiple adlayers on flat or stepped substrates with different symmetry characteristics. Adlayers can be assembled using individual atoms at different interatomic distances and can be easily translated or rotated in any direction at the substrate surface, which is the fundamental algorithm in our approach.

For the first time, the USP model was shown to work for detailed characterization of the iodine adlayer on the Pt(111) surface.[10] Simulation was carried out in a wide range of adlayer coverages, and it could completely reproduce the experimental findings for all known structures. Although it is based on a simple geometrical approach, we found that it allows the development of detailed structural models and better understanding of the mechanism of adlayer formation. In this first study, we found that the *minimum average adsorbate height* is the crucial and sufficient condition (parameter) to identify and describe the most stable structures of the iodine adlayer on the Pt(111) surface. Indeed, it was the only parameter needed to describe the hexagonally ordered iodine adlayer on the Pt(111) surface.

The model for the I−Au(111) system consists of two layers of spheres. The substrate layer is arranged in hexagonal order [Au(111) surface], and the adsorbate layer possesses c($p\times\sqrt{3}$)-*R*30° symmetry. The Au(111) surface is represented by close-packed hexagonally ordered spheres of radius $R_{Au} = 1.44$ Å. The iodine adlayer consists of smaller spheres ordered in a c($p\times\sqrt{3}$)*R*30° pattern with $R_I = 1.33$ Å, a value which corresponds to the iodine covalent radius.[36] In the figures presented in our paper, iodine is shown by circles with a larger radius, just for practical reasons. In our model, the *p* value was varied between 2.3 and 3. This *p* range corresponds to the interval of adlayer coverage from $\theta = 0.333$ to $\theta = 0.435$. Note that the change of *p* is related to the change in the intersphere distance along the *X* direction of the gold substrate, while the intersphere distance in the $\sqrt{3}$ direction is always the same (4.99 Å). Under these restrictions, the adlayer spheres never touch each other.

In the process of simulation, the iodine adlayer was translated all over the (111) surface. After each shift, a detailed analysis of the atomic registry and the geometric characterization of the adlayer was carried out. This process was repeated for each

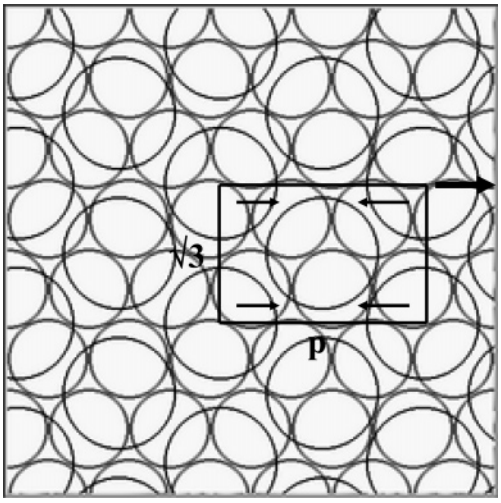

Figure 1. Illustration of the c($p\times\sqrt{3}$)R30° adsorbate adlayer (large balls) shifting over the hexagonal substrate surface (small balls). The p-bisector direction is marked by an arrow.

value of p (uniaxial compression) maintaining rigid hexagonal (substrate) and c($p\times\sqrt{3}$)R30° (adsorbate) symmetry. As a result of such simulation, numerous structural patterns were generated. To identify structures which have the same characteristics as those reported in experiments,[13] we impose two conditions as selective criteria: minimization of the adlayer distance from the substrate (minimum average adsorbate height, A) (eq 2) and the adlayer flatness condition or minimization of the height difference between adjacent spheres (minimum roughness, R) (eq 3).

The height of each adsorbate sphere (Z) is calculated in the surface-normal direction according to eq 1.

$$Z = \sqrt{(r_1 + r_2)^2 - (x_a - x_s)^2 - (y_a - y_s)^2} \qquad (1)$$

where r_1 and r_2 are the substrate and adsorbate radii, respectively, (x_a, y_a) is the adsorbate sphere position, and (x_s, y_s) is the closest substrate sphere position.

$$A(P) = \sum_{i=1}^{N} Z(P_i)/N \qquad (2)$$

$$R(P) = \sqrt{\frac{\sum_{i=1}^{N} (Z(P_i) - A(P))^2}{N}} \qquad (3)$$

where P represents a configuration of adsorbate spheres (N particles) and the summation goes over all spheres in P. For more details, see ref 10. Note the agreement between these equations and the definition of *mean* and *standard deviation* in mathematical statistics.[37]

One should notice that such a procedure is different from the one that was used for the simulation of the I−Pt(111) system, because of the second parameter, the minimum roughness (R).

Results and Discussion

The simulation starts by creating the c($p\times\sqrt{3}$)R30° unit cell of the iodine adlayer with characteristics known from the literature[13,25] (see Figure 1). The iodine adlayer was translated (shifted) over the Au(111) surface in all directions with close monitoring of the change in the iodine adatom registry. Shifting was performed via small increments in order to achieve reasonable precision in the simulation. The adatom movement is collective, since all adatoms follow the same direction of shifting. Note that, after shifting in any direction, the symmetry of the c($p\times\sqrt{3}$)R30° unit cell is completely preserved. After each adlayer translation, in particular after translations along the p-bisector direction, changes in the atomic corrugation were evaluated. As an output of the simulation, a large number of c($p\times\sqrt{3}$)R30° structures for each value of p, located at different positions on the Au(111) substrate (due to shifting), were observed. To select iodine structures which possess similar characteristics to those observed in experiments (flat adlayers observed by STM with uniform registry close to bridge position, on average 2.3−2.4 Å from the substrate surface),[13] two parameters have been imposed in our model during the selection process.

In the first run, as presented in Figure 2, among all simulated c($p\times\sqrt{3}$)R30° patterns (p between 2.3 and 3.05), we have been looking for those that on average are closest to the Au(111) substrate. The closest structures for unrestricted XY plane movement are presented by the dashed line. The adatom registry for several chosen patterns on the minimum average height line is presented. For $p = 3$, the c($p\times\sqrt{3}$)R30° pattern could be identified as hexagonally ordered ($\sqrt{3}\times\sqrt{3}$)R30°, with all iodine adatoms in the 3-fold site and as close as possible to the substrate. However, when p is less than 3, c($p\times\sqrt{3}$)R30° structures are similar to those found in experiments, with an average distance of 2.44 Å from the substrate and with all adatoms on sites with similar registry.

In an additional simulation, the c($p\times\sqrt{3}$)R30° arrangement was shifted exclusively along the p-bisector direction (solid line in Figure 2). It can be clearly seen that changing p does not induce changes in the average height and adlayer atomic registry, as long as translation is restricted along the p-bisector direction. Also, very interestingly, by strictly keeping restriction of movement exclusively along the p-bisector, in the case of $p = 3$, the simulation shows the existence of a structure with ($\sqrt{3}\times\sqrt{3}$)R30° symmetry which is very much farther from the surface, with iodine adatoms in the bridge site, rather than 3-fold sites. Another interesting discrepancy is found for c($p\times\sqrt{3}$)-R30° with $p = 2.5$, which appears slightly closer (0.025 Å) to the substrate than other structures of the same pattern. According to our understanding, such particular structure has more possibilities to be formed than other ones. Even from this simple plot, and taking into account that the atomic registry of all iodine adatoms is very similar, one could see why c($p\times\sqrt{3}$)R30°−I−Au(111) appears "atomically flat" in STM images.[24,25] Note that the vertical resolution of the STM technique is limited to 0.05 Å. Taking into account this experimental finding, our system was subjected to fulfill an additional criterion: the requirement that the iodine adlayer maintains minimum roughness during shifting over the substrate (minimum difference in the atomic corrugation).

Figure 3 shows the results of the simulation when an adlayer with c($p\times\sqrt{3}$)R30° structure was moved exclusively along the p-bisector (solid line) and in the XY plane (dashed line). In all cases, structures with minimum roughness (0.032 Å) were obtained when the adlayer was shifted along the p-bisector direction. Indeed, for $p = 2.5$ and $p = 3$, the roughness diminished even more, what we believe is the result of very specific adatom registry. Further work is in progress to understand the mechanism of transformation between ($\sqrt{3}\times\sqrt{3}$)-R30° and c($p\times\sqrt{3}$)R30° patterns.

The differences between values for the maximum roughness of the iodine adlayer translated in the XY plane (dashed line)

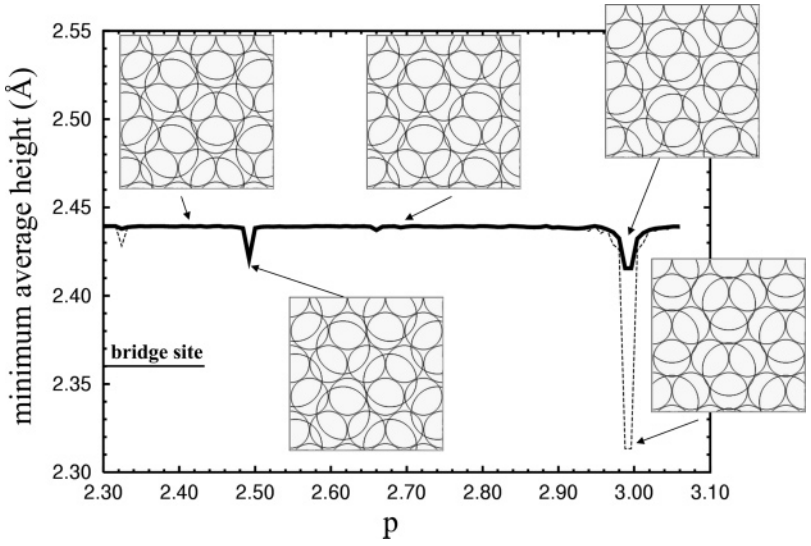

Figure 2. Comparison of the minimum average height for all c($p\times\sqrt{3}$)*R*30° structures with 2.3 < p < 3.05. The bold line shows the minimum average height when iodine adatoms were shifted along the *p*-bisector exclusively, while the dashed line shows the same parameter for unrestricted shifting in the *XY* plane of the substrate.

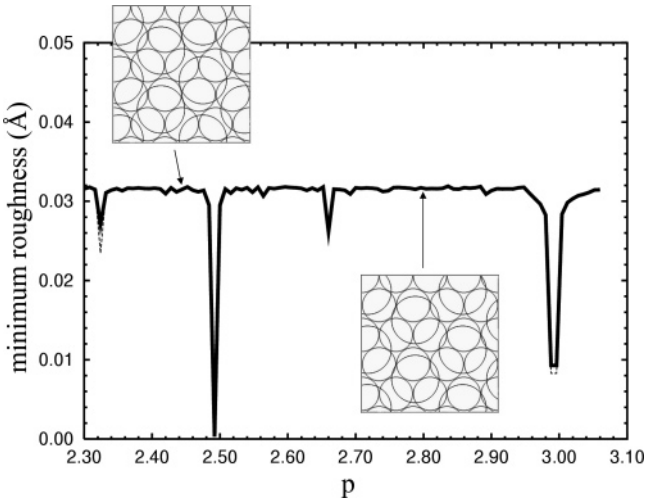

Figure 3. Comparison of the minimum roughness for all c($p\times\sqrt{3}$)-*R*30° structures with 2.3 < p < 3.05. The bold line shows the minimum roughness when the iodine adatoms were shifted along the *p*-bisector exclusively, while the dashed line shows the same parameter for unrestricted shifting in the *XY* plane of the substrate.

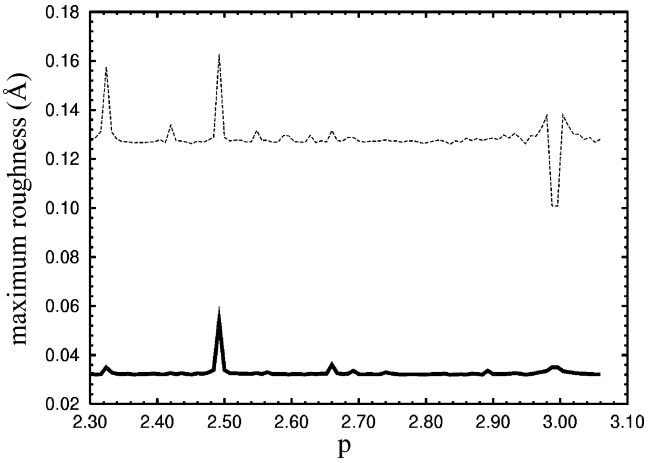

Figure 4. Comparison of the maximum roughness between all c($p\times\sqrt{3}$)*R*30° structures with 2.3 < p < 3.05. The bold line shows the maximum roughness when the iodine adatoms were allowed to shift along the *p*-bisector exclusively, while the dashed line shows this parameter for unrestricted shifting in the *XY* plane of the substrate. Note that the structures with the lowest roughness are those with adatoms positioned in the *p*-bisector direction.

and along the *p*-bisector (solid line) direction are presented in Figure 4. One can clearly see that the translation of the iodine adlayer over the substrate out of the *p*-bisector direction could lead to the formation of patterns with significantly larger roughness. However, the minimum value of the maximum roughness is achieved only during the shifting along the *p*-bisector direction, as a preferential route. As demonstrated in Figures 3 and 4 (solid line), only the iodine adlayers aligned along the *p*-bisector keep minimum corrugation (less than 0.035 Å). Note, for compression routes different than the *p*-bisector, the iodine adlayer will possess a higher roughness and will be farther from the substrate. Therefore, one could define the meaning of the *p*-bisector as a special pathway for iodine adatom movement during the compression phenomena on the Au(111) surface, which allows the transformation of the c($p\times\sqrt{3}$)*R*30° iodine adlayer with minimum changes in adlayer corrugation and distance from the substrate. It would be very interesting to know if other systems which show adlayer compression phenomena also present *p*-bisector routes.

Figure 5 shows a three-dimensional graph of the average height (a) and roughness (b) for unrestricted *XY* movement for $p = 2.5$ as a function of the *X* and *Y* positions. It demonstrates that, in the case of selected structures found along the *p*-bisector, both criteria (minimum average height and minimum roughness) are fulfilled simultaneously. We believe that a second additional parameter, the minimum roughness, is directly related to the magnitude of lateral interactions between the iodine adatoms on the Au(111) surface. However, to verify this hypothesis and understand the difference between I−Au(111) and I−Pt(111), calculation of the adsorption energy by quantum mechanical methods is required and in progress.

Note that if the minimum average height is used exclusively as a selective parameter in the simulation, the hexagonally ordered ($\sqrt{3}\times\sqrt{3}$)*R*30°, ($\sqrt{7}\times\sqrt{7}$)*R*19.1°, and (3×3) structures found for I−Pt(111) will be the most stable ones.[10] Therefore, the simultaneous use of two parameters is required for correct characterization of the I−Au(111) system.

Following this line, we compare two sets of structures: iodine adlayer with hexagonal order, obtained on Pt(111) [including ($\sqrt{3}\times\sqrt{3}$)*R*30°, ($\sqrt{7}\times\sqrt{7}$)*R*19.1°, and (3×3)], and iodine

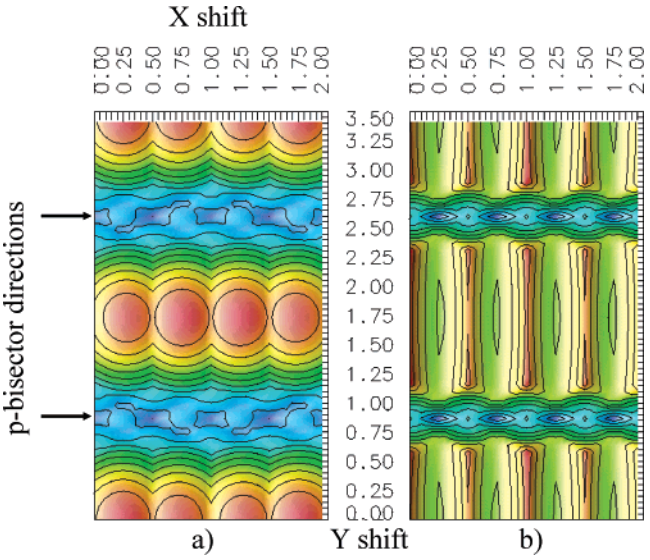

Figure 5. Three-dimensional plot of the average height and roughness changes as a function of the adlayer shifting in the *XY* plane of the substrate. The structures with the lowest average height and the lowest roughness (corrugation) are obtained while shifting along the *p*-bisector (marked by arrows).

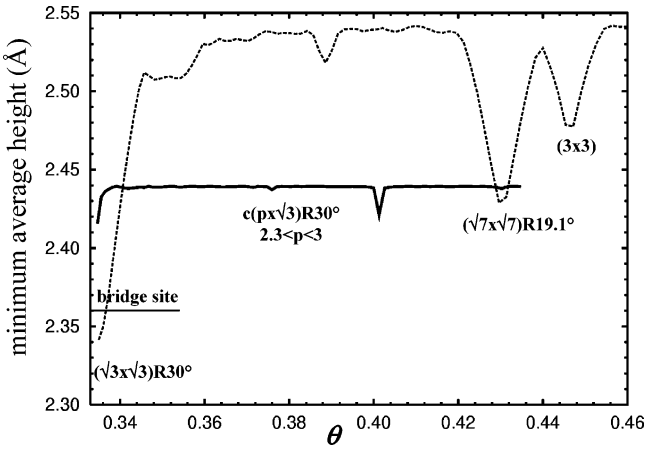

Figure 6. Comparison of the minimum average height between c($p\times\sqrt{3}$)*R*30° structures on the *p*-bisector direction [I−Au(111] and characteristic hexagonal arrangements of iodine on Pt(111). The bold line shows the minimum average height for c($p\times\sqrt{3}$)*R*30° structures, while the dashed line shows this parameter for hexagonal structures.

adlayer with centered-rectangular c($p\times\sqrt{3}$)*R*30° structures, observed for iodine on Au(111) in a large range of surface coverages (0.33−0.46). In both adlayers, the same iodine radius was used. Comparison is based on the analysis of two parameters: minimum average height (Figure 6) and maximum roughness (Figure 7). With respect to the minimum average height, all c($p\times\sqrt{3}$)*R*30° structures are equally close to the Au(111) substrate and, in general, much closer than the hexagonal iodine adlayer on Pt(111). Difference is mainly in the range of 0.1 Å, except some specific points. The most commonly observed iodine adlayers on Pt(111) with ($\sqrt{3}\times\sqrt{3}$)-*R*30°, ($\sqrt{7}\times\sqrt{7}$)*R*19.1°, and (3×3) symmetry are equal or even closer to the substrate than c($p\times\sqrt{3}$)*R*30° structures on the *p*-bisector. Figure 7 shows that iodine adlayer formation via hexagonal arrangement induces significant changes in the adlayer corrugation. Contrary, in the case of the c($p\times\sqrt{3}$)*R*30° iodine adlayer along the *p*-bisector, adlayers with minimum corrugation are dominant. Furthermore, we compare two particular iodine adlayers: centered-rectangular c($p\times\sqrt{3}$)*R*30° with $p = 2.33$ on Au(111) and hexagonal ($\sqrt{7}\times\sqrt{7}$)*R*19.1° on

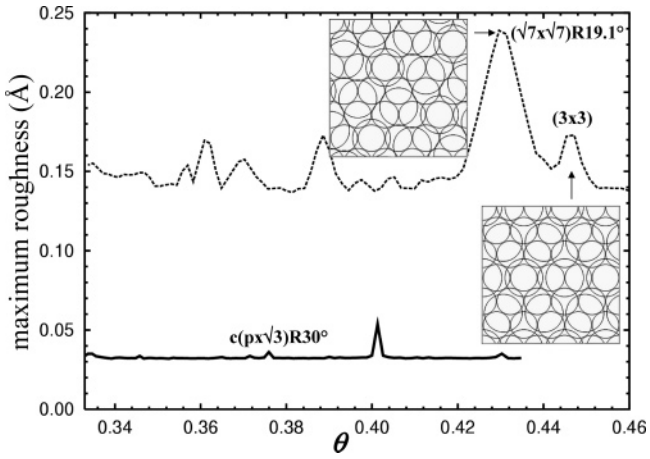

Figure 7. Comparison of the maximum roughness between c($p\times\sqrt{3}$)-*R*30° structures on the *p*-bisector and hexagonal structures. The bold line shows the maximum roughness for c($p\times\sqrt{3}$)*R*30° structures in the *p*-bisector, while the dashed line shows this parameter for hexagonal structures.

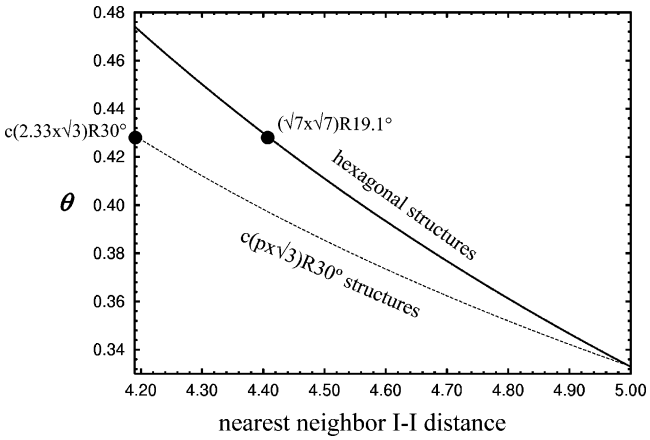

Figure 8. Plot of surface coverage (θ) vs nearest-neighbor distance for c($p\times\sqrt{3}$)*R*30° and hexagonal structures. Both curves intersect at the ($\sqrt{3}\times\sqrt{3}$)*R*30° structure.

Pt(111) with the same surface coverage. As is clear from Figure 8, these two arrangements possess different nearest-neighbor distances between the iodine adatoms due to their different adlayer symmetries. Both c(2.33×$\sqrt{3}$)*R*30° and ($\sqrt{7}\times\sqrt{7}$)-*R*19.1° patterns were translated over the substrate surface in the process of simulation. After each translation step, the adsorbate average height and roughness were calculated to construct the graph on Figure 9. Note that each cross in this graph is associated to separate pattern with ($\sqrt{7}\times\sqrt{7}$)*R*19.1° symmetry. This graph shows that the hexagonally ordered ($\sqrt{7}\times\sqrt{7}$)*R*19.1° adlayer could be formed under a variety of conditions: far from the surface but with minimum corrugation (left) or closer to the surface (2.4 Å) and with larger corrugation (right).

Simulation of the c(2.33×$\sqrt{3}$)*R*30° iodine adlayer on Au(111) indicates significantly different behavior. Despite translation over the substrate (resticted along the *p*-bisector), the iodine adlayer maintains the same average distance from the substrate and the same roughness (Figure 9).

Comparison between c(2.33×$\sqrt{3}$)*R*30° and ($\sqrt{7}\times\sqrt{7}$)*R*19.1° shows that c(2.33×$\sqrt{3}$)*R*30° is less corrugated than any of the ($\sqrt{7}\times\sqrt{7}$)*R*19.1° arrangements, and in most cases closer to the substrate. The hexagonally ordered ($\sqrt{7}\times\sqrt{7}$)*R*19.1° adlayer could not be at the same time close to the substrate and very flat. To be closer to the surface, it needs to increase its adlayer roughness.

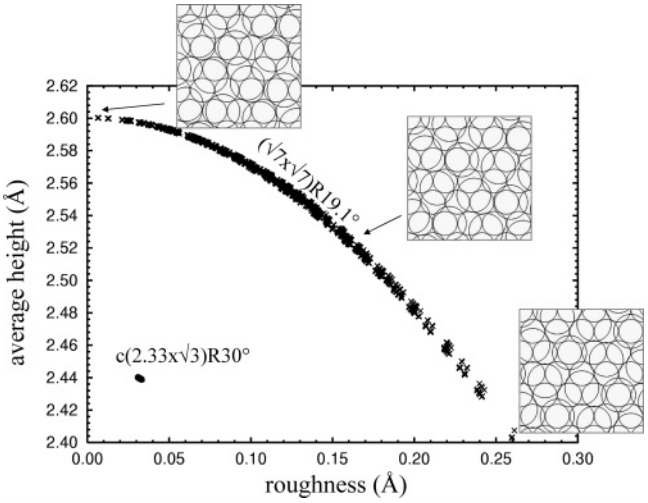

Figure 9. Average adlayer height vs adlayer roughness plot for the $(\sqrt{7}\times\sqrt{7})R19.1°$ structure and the c($p\times\sqrt{3}$)$R30°$ structure with $p = 2.33$. Both structures possess the same degree of coverage.

It could be very interesting, from the aspect of modern nanoelectronics and construction of atomic devices, for which functionality depends on the position and distance between atomic adlayers, to understand how a certain type of adlayer could be transformed into another one. In this way, adlayers with the same surface coverage but different and desired properties could be designed in the future.

Conclusions

A simple unequal-sphere packing model, based on geometrical principles, was used to simulate the centered-rectangular c($p\times\sqrt{3}$)$R30°$ adlayer on the Au(111) surface. Results of our study clearly show that the USP model could be used successfully for detailed characterization of c($p\times\sqrt{3}$)$R30°$ structures, including description of the iodine adatom registry and the uniaxial compression phenomenon. The simulation was based on two conditions: minimization of the adsorbate average height (minimum adlayer distance from the substrate) and minimization of the adlayer roughness (minimum adlayer corrugation). The c($p\times\sqrt{3}$)$R30°$ arrangements in the p range from 2.3 to 3.0, closest to the substrate and, at the same time, with minimum roughness, were equal to those found in SXS, LEED, and STM studies. For this specific set of c($p\times\sqrt{3}$)$R30°$ structures, we found that iodine adatoms are positioned on the gold surface p-bisector. Indeed, one could also see from our study that during uniaxial compression of the c($p\times\sqrt{3}$)$R30°$ pattern, iodine adatoms move along the p-bisector directions. Any other movement, out of the p-bisector direction, which was also carefully investigated in our study, produces patterns with higher corrugation or distanced farther from the substrate. From the comparison between hexagonal and centered-rectangular iodine arrangements on Au(111), we could clearly see the difference in the adatom registry for these two types of adlayer arrangements. In the case of the hexagonal arrangement, iodine adlayers undergo severe changes in roughness and average adsorbate height. The obtained results are of special importance for understanding adatom (anion) behavior on different substrates, such as Au(111) versus Pt(111). On the other hand, understanding of adlayer transformation processes could be of special interest for the development of modern electronics. From this point of view, our simple USP model appears to be a rather useful tool.

Acknowledgment. The authors wish to gratefully acknowledge support by CONACYT (fellowship for A.T.), UAM-Iztapalapa Division de Ciencia Basica e Ingenieria, and Instituto Mexicano del Petroleo (IMP), project FIES-98-100-I.

References and Notes

(1) Hubbard, A. T. *Chem. Rev.* **1988**, *88*, 636.

(2) Somorjai, G. A. *Introduction to Surface Chemistry and Catalysis*; John Wiley & Sons: New York, 1994.

(3) Magnussen, O. M. *Chem. Rev.* **2002**, *102*, 679.

(4) Kolb, D. M. *Physical and Electrochemical Properties of Metal Monolayers on Metallic Substrates*; John Wiley: New York, 1978; p 125.

(5) Kolb, D. M. *Prog. Surf. Sci.* **1996**, *51*, 109.

(6) Gewirth, A. A.; Niece, B. K. *Chem. Rev.* **1997**, *97*, 1129.

(7) Chang, S. C.; Yau, S.-L.; Schardt, B. C.; Weaver, M. J. *J. Phys. Chem.* **1991**, *95*, 4787.

(8) Frank, D. G.; Chyan, O. M. R.; Golden, T.; Hubbard, A. T. *J. Phys. Chem.* **1993**, *97*, 3829.

(9) Labayen, M.; Furman, S. A.; Harrington, D. A. *Surf. Sci.* **2003**, *525*, 149.

(10) Tkatchenko, A.; Batina, N. *Phys. Rev. B* **2004**, *70*, 195403.

(11) Tkatchenko, A.; Batina, N.; Cedillo, A.; Galvan, M. *Surf. Sci.* **2005**, *581*, 58.

(12) Toney, M. F.; Gordon, J. G.; Samant, M. G.; Borges, G. L.; Wiesler, D. G.; Yee, D.; Sorenson, L. B. *Langmuir* **1991**, *7*, 796.

(13) Ocko, B. M.; Watson, G. M.; Wang, J. *J. Phys. Chem.* **1994**, *98*, 897.

(14) Yau, S.-L.; Vitus, C. M.; Schardt, B. C. *J. Am. Chem. Soc.* **1990**, *112*, 3677.

(15) Yau, S.-L.; Gao, X.; Chang, S. C.; Schardt, B. C.; Weaver, M. J. *J. Am. Chem. Soc.* **1991**, *113*, 6049.

(16) Gao, X.; Weaver, M. J. *J. Am. Chem. Soc.* **1992**, *114*, 8544.

(17) Tao, N. J.; Lindsay, S. M. *J. Phys. Chem.* **1992**, *96*, 5213.

(18) Ocko, B. M.; Wang J. Surface Structure at the Au(111) Electrode. In *Synchrotron Techniques in Interfacial Electrochemistry*; Melendres, C. A., Tadjeddine A., Eds.; Kluwer Academic Publishers: Dordrecht, 1994; pp 127−155.

(19) Itaya, K.; Batina, N.; Kunitake, M.; Ogaki, K.; Kim, Y.-G.; Wan, L.-J.; Yamada, T. In *Solid−Liquid Electrochemical Interfaces*; Jerkiewicz, G., Soriaga, G. M. P., Uosaki, K., Wieckowski, A., Eds.; ACS Symposium Series 656; American Chemical Society: Washington, DC, 1995.

(20) Ocko, B. M.; Magnussen, O. M.; Wang, J. X.; Adzic, R. R. *Physica B* **1996**, *221*, 238.

(21) Yamada, T.; Ogaki, K.; Okubo, S.; Itaya, K. *Surf. Sci.* **1996**, *369*, 321.

(22) Yamada, T.; Batina, N.; Ogaki, K.; Ocubo, S.; Itaya, K. In Proceedings of the Sixth International Symposium on Electrode Processes; Wieckowski, A., Itaya, A., Eds.; The Electrochemical Soc. Inc.: Pennington, NY, 1996; Vol. 96-8, p 43.

(23) Nagatani, Y.; Hayashi, T.; Yamada, T.; Itaya, K. *Jpn. J. Appl. Phys.* **1996**, *35*, 720.

(24) Yamada, T.; Batina, N.; Itaya, K. *Surf. Sci.* **1995**, *335*, 204.

(25) Batina, N.; Yamada, T.; Itaya, K. *Langmuir* **1995**, *11*, 4568.

(26) Cochran, S. A.; Farrell, H. H. *Surf. Sci.* **1980**, *95*, 359.

(27) Huang, L.; Zeppenfeld, P.; Horch, S.; Comsa, G. *J. Chem. Phys.* **1997**, *107*, 585.

(28) Magnussen, O. M.; Ocko, B. M.; Wang, J. X.; Adzic, R. R. *J. Phys. Chem.* **1996**, *100*, 5500.

(29) Magnussen, O. M.; Ocko, B. M.; Adzic, R. R.; Wang, J. X. *Phys. Rev. B* **1995**, *51*, 5510.

(30) Wang, X.; Chen, R.; Wang, Y.; He, T.; Liu, F. C. *J. Phys. Chem. B* **1998**, *102*, 7568.

(31) Kunitake, M.; Batina, N.; Itaya, K. *Langmuir* **1995**, *11*, 2337.

(32) Batina, N.; Kunitake, M.; Itaya, K. *J. Electroanal. Chem.* **1996**, *405*, 245.

(33) Ogaki, K.; Batina, N.; Kunitake, M.; Itaya, K. *J. Phys. Chem.* **1996**, *100*, 7185.

(34) Kunitake, M.; Akiba, U.; Batina, N.; Itaya, K. *Langmuir* **1997**, *13*, 1607.

(35) Tkatchenko, A.; Batina, N. *J. Chem. Phys.* **2005**, *122*, 094705.

(36) Pauling, L. C. *The Nature of the Chemical Bond*, 3rd ed.; Cornell University Press: Ithaca, NY, 1960.

(37) Mendenhall, W.; Scheaffer, R. L.; Wackerly, D. D. *Mathematical Statistics with Applications*, 4th ed.; PWS-KENT Publishers: Boston, 1990.